

# Modeling Double Charge Exchange processes occurring in Heavy Ion Reactions

Jessica Ilaria Bellone<sup>1,2</sup>, Maria Colonna<sup>2,\*</sup>, Danilo Gambacurta<sup>2</sup>, and Horst Lenske<sup>3</sup>  
(NUMEN collaboration)

<sup>1</sup>Università degli studi di Catania, Dipartimento di Fisica e Astronomia “E. Majorana”, via Santa Sofia 64, 95123 Catania CT, Italy.

<sup>2</sup>Laboratori Nazionali del Sud, INFN, I-95123 Catania, Italy.

<sup>3</sup>Institut für Theoretische Physik, Justus-Liebig-Universität Giessen, D-35392 Giessen, Germany.

**Abstract.** Heavy ion induced double charge exchange reactions are treated as an incoherent sequence of two reactions driven by the exchange of charged mesons (double single charge exchange, DSCE). The process is described within a fully quantum mechanical distorted wave 2-step theory (2nd order DWBA). The DSCE reaction amplitudes are shown to be separable into superpositions of distortion factors, accounting for initial and final state ion-ion elastic interactions, and nuclear matrix elements (NMEs). Explicit expressions of projectile and target NMEs are derived within the QRPA theory. Reduction schemes for the DSCE transition form factors are described, analyzing their momentum structure within the closure approximation. Formal analogies between the NMEs involved in DSCE reactions and in double beta decays are also pointed out. Results, obtained within this theoretical framework, are illustrated for the reaction  $^{40}\text{Ca} (^{18}\text{O}, ^{18}\text{Ne})^{40}\text{Ar}$  at 15.3 AMeV and compared to the data measured at INFN-LNS by the NUMEN Collaboration. Furthermore, preliminary results for reactions involving heavier systems, such as  $^{76}\text{Se} (^{18}\text{O}, ^{18}\text{Ne})^{76}\text{Ge}$ , are shown.

## 1 Introduction

Nuclear charge exchange transitions are processes characterized by the change of the nuclear charge by one or more units, while keeping the mass number constant. These transitions can be spontaneous or external-field-induced processes. The former include weak decays ( $\beta$ ,  $\beta\beta$  decays), while the latter comprise reactions induced by the nuclear strong interaction (charge-exchange reactions). The study of nuclear charge-changing transitions allows to gain information useful for different fields of physics, from astrophysics to nuclear and particle physics. Nowadays, double charge-exchange (DCE) nuclear reactions, i.e.  $a(N, Z) + A(N, Z) \rightarrow b(N \pm 2, Z \mp 2) + B(N \mp 2, Z \pm 2)$  transitions, are attracting increasing interest. Indeed, such reactions are used to probe spin and isospin components of NN interaction potential and to study exotic nuclear systems, such as the tetra-neutron system through the double charge-exchange reaction  $^4\text{He}(^8\text{He}, \alpha\alpha)4n$  [1]. In particular, the recent development of high resolution experiments led to a renewed interest in heavy ion induced DCE reactions

---

\*e-mail: colonna@lns.infn.it

(HIDCE), because this kind of reactions could offer the possibility to explore new collective modes of nuclear matter (e.g. DIAS and the not yet observed DGTGR) and to provide data-driven information on  $0\nu\beta\beta$  decay nuclear matrix elements. Concerning the latter topic, the NUMEN collaboration (LNS, Catania) studies HIDCE reactions with the aim of constraining the nuclear matrix elements (NMEs) involved in  $0\nu\beta\beta$  decay from measurements of HIDCE cross sections [2]. The latter is a theorized weak decay characterized by the emission of two charged leptons with no neutrino emission,  $A(N, Z) \rightarrow A(N \pm 2, Z \mp 2) + 2e^\pm$ ; it is worth noting that this decay is not allowed within the Standard Model of particle physics, because it would imply total lepton number violation ( $\Delta L = 2$ ). Moreover,  $0\nu\beta\beta$  decay would happen only if neutrinos have non-zero mass and are Majorana particles, meaning that they are their own anti-particle. The observation of  $0\nu\beta\beta$  decay would allow to shed light on physics beyond the Standard Model and also on the origin of matter-antimatter asymmetry in the Universe. An accurate estimate of  $0\nu\beta\beta$  NMEs is of fundamental importance to get a reliable prediction of the decay half-life. Hitherto, the numerous attempts made for evaluating these NMEs, using several theoretical approaches, at various levels of sophistication, led to results still showing significant discrepancies [3]. In this respect, HIDCE reactions turn out to be an interesting tool to infer data-driven information on double-beta decay NMEs. A first step towards the feasibility of this kind of studies is represented by the existence of a linear correlation between the NMEs of DGT-DCE reactions and  $0\nu\beta\beta$  decay, proved by different nuclear structure models [4, 5].

HIDCE nuclear reactions can be fed by two reaction mechanisms:

- a sequence of (correlated or uncorrelated) exchange of charged mesons (direct or hard processes);
- sequential multi-nucleon transfers feeding DCE (mean-field or soft processes)[6, 7].

The present work focuses on the former reaction mechanism, which is the one allowing to describe HIDCE reactions by means of the same spin-isospin transition operator involved in double beta decays, thus allowing to recover analogies between these processes.

Direct HIDCE reactions can be described as a sequence of two uncorrelated SCE reactions (each one induced by charged-meson exchange), i.e. as a two-step process (Double Single Charge Exchange, DSCE). Correlations between the two SCE reactions can also be accounted for, thus leading to the description of an effective-one-step process (Majorana-like reaction mechanism, MDCE) [8]. In these proceedings, we focus on the DSCE reaction mechanism. In [9], it is proved that DSCE and  $2\nu\beta\beta$  NMEs show similar structures, even if the former is characterized by a considerable more complex multipole and spin structure. Moreover, noting that both DSCE reactions and  $0\nu\beta\beta$  decay involve the same nuclear states in the (off-shell) intermediate channel, a possible connection can exist also between these processes.

A further step toward the extraction of data-driven information on double beta decay NMEs, is given by the possibility to factorize the HIDCE cross section [9], allowing to disentangle the information concerning projectile and target nuclear structure from reaction dynamics. However, the formalism outlined in [9, 10] does not provide a connection among the DSCE cross section and projectile and target DSCE NMEs, separately. Hence, an extension of the formalism is necessary in order to disentangle projectile and target nuclear structure information. The formalism allowing to reach this goal is discussed below.

## 2 The s-channel formalism

The heavy ion DSCE cross section is treated within second order DWBA. This theoretical framework allows to express the DSCE transition matrix element (TME) as the convolution

of two SCE TMEs, and the Green function,  $G_\gamma$ , accounting for the (free) propagation of the nuclear system generated by the first SCE reaction, as already shown in [9] (t-channel representation). A proper rotation in angular momentum space allows to decouple projectile and target angular momenta involved in the two-step transition (s-channel representation) [10].

After performing this unitary transformation and by properly treating the nuclear states populating the intermediate channel within the closure approximation, the DSCE TME can be written as

$$\mathcal{T}(\mathbf{k}_\alpha, \mathbf{k}_\beta) \simeq \sum_{c,C} \sum_{S,M} (-1)^{S-M} \int d^3 q_1 \int d^3 q_2 \left[ F_{S_2}^{BC}(\mathbf{q}_2) F_{S_1}^{CA}(\mathbf{q}_1) \right]_{SM} \left[ F_{S_2}^{bc}(\mathbf{q}_2) F_{S_1}^{ca}(\mathbf{q}_1) \right]_{S-M} V_{S_2 T}(\mathbf{q}_2) V_{S_1 T}(\mathbf{q}_1) N_{\alpha\beta}(\mathbf{q}_1 + \mathbf{q}_2) \quad (1)$$

where  $N_{\alpha\beta}(\boldsymbol{\eta})$  is the DSCE distortion factor,  $V_{ST}(\mathbf{q})$  is the Fourier transform of the NN interaction terms and the  $F_{S_i}^{(XY)}(\mathbf{q})$  terms represent the Fourier transform of projectile (lower case apices) and target (upper case apices) one-body transition densities, embedding information on the reduced matrix element of the SCE transition operator and accounting for first ( $i=1$ ) and second ( $i=2$ ) SCE transition. The propagator is not shown in (1), because it reduces to a constant term, owing to the closure approximation. Eq. (1) shows projectile and target transition densities still entangled. Hence, in order to separately access these transition densities, i.e. the DSCE NMEs of the two interacting nuclei, further approximations are necessary. For this purpose, after a simple change of integration variables ( $\boldsymbol{\eta} = \mathbf{q}_1 + \mathbf{q}_2$  and  $\boldsymbol{\xi} = \mathbf{q}_1 - \mathbf{q}_2$ ), the following two approximations are used:

- average- $\rho$  approximation

$$\tilde{\rho}_T^{2BTD}(\boldsymbol{\eta}) \equiv \sum_C \frac{(2\pi)^3}{V_\xi} \int d^3 r e^{i\boldsymbol{\eta}\cdot\mathbf{r}} \left[ F_{S_2}^{(BC)}(\mathbf{r}) F_{S_1}^{(CA)}(\mathbf{r}) \right]_{SM} \quad (2)$$

where the above simple expression of target 2-body transition density (2BTD) is obtained averaging the product of the Fourier transforms of first and second step SCE one-body transition densities (OBTDS) over the half-off-shell linear momentum transfer  $\xi$  (the same expression is found for projectile 2BTD).  $V_\xi$  is a normalization factor with the dimensions of a volume in momentum space, that allows to recover the correct dimension of the 2BTDs.

- collinear approximation

$$\tilde{\rho}_T^{2BTD}\left(\frac{\boldsymbol{\eta}}{2}\right) \equiv \sum_C F_{S_2}^{(BC)}\left(\frac{\boldsymbol{\eta}}{2}\right) F_{S_1}^{(CA)}\left(\frac{\boldsymbol{\eta}}{2}\right) \frac{V_\eta}{V_\xi} \equiv \sum_C F_{S_2}^{(BC)}\left(\frac{\boldsymbol{\eta}}{2}\right) F_{S_1}^{(CA)}\left(\frac{\boldsymbol{\eta}}{2}\right) f_{coll} \quad (3)$$

where only the contribution from  $\xi = 0$ , is considered for each of the two SCE OBTDS, i.e. equal momenta transfers are assumed in the two SCE reactions. Here,  $f_{coll}$  is a dimensionless normalization factor used to scale results to the  $\theta = 0$  value of the angular distribution obtained in t-channel.

Within both approximations, the remaining integral over  $\xi$ , in eq. (1), allows to get the following quite simple expression of the DSCE NN interaction potential

$$V_{S_1 S_2 T}^{DSCE}(\boldsymbol{\eta}) \equiv (2\pi)^3 \int d^3 r V_{S_1 T}(\mathbf{r}) V_{S_2 T}(\mathbf{r}) e^{i\boldsymbol{\eta}\cdot\mathbf{r}} \quad (4)$$

In this way, both collinear and average- $\rho$  approximations lead to the following single-step like expression of the DSCE TME,

$$\mathcal{T}(\mathbf{k}_\alpha, \mathbf{k}_\beta) \simeq \int d^3 \eta \tilde{\rho}_p^{2BTD}\left(\frac{\boldsymbol{\eta}}{x}\right) \tilde{\rho}_T^{2BTD}\left(\frac{\boldsymbol{\eta}}{x}\right) V_{S_1 S_2 T}^{DSCE}(\boldsymbol{\eta}) N_{\alpha\beta}(\boldsymbol{\eta}) \quad (5)$$

where  $x = 1$  for average- $\rho$  approximation and  $x = 2$  for collinear approximation. For a TME expression like that of eq. (5) it is possible to get a factorised expression for small momentum transfer values [11], leading in turn to the following factorized DSCE cross section expression

$$\frac{d\sigma}{d\Omega} \simeq_{\eta \ll 1} |\tilde{\rho}_P^{2BTD}(\frac{\mathbf{k}_{\alpha\beta}}{x})|^2 |\tilde{\rho}_T^{2BTD}(\frac{\mathbf{k}_{\alpha\beta}}{x})|^2 |V_{S_1 S_2 T}^{DSCE}(\mathbf{k}_{\alpha\beta})|^2 |\tilde{n}_{\alpha\beta}(\mathbf{k}_{\alpha\beta})|^2, \quad (6)$$

where the distortion coefficient  $\tilde{n}_{\alpha\beta}(\mathbf{k}_{\alpha\beta})$  is defined by the relation  $N_{\alpha\beta}(\boldsymbol{\eta}) = \delta(\boldsymbol{\eta} - \mathbf{k}_{\alpha\beta}) \tilde{n}_{\alpha\beta}(\mathbf{k}_{\alpha\beta})$ . Eq. (6) is a crucial step toward inferring data-driven information on DCE NMEs.

### 3 Results

To assess the quality of the approximations discussed in section 2, s-channel results are compared to calculations obtained within the t-channel representation (i.e. results obtained within the formalism described in [9]). Here, the results for the test reaction  $^{40}\text{Ca}(^{18}\text{O}, ^{18}\text{Ne}_{gs})^{40}\text{Ar}_{gs}$  are illustrated (fig. 1), together with preliminary results for the reaction  $^{76}\text{Se}(^{18}\text{O}, ^{18}\text{Ne}_{gs})^{76}\text{Ge}_{gs}$  (figs. 2 and 3), studied within the NUMEN collaboration.

Initial and final state interactions are properly accounted for by means of São Paulo optical potentials [12] with parameters suitably tuned through the standard analysis of elastic and inelastic channel experimental angular distributions [13, 14].

Fig. 1 illustrates that, for the test system  $^{40}\text{Ca} + ^{18}\text{O}$ , the average- $\rho$  approximation allows to reproduce both the order of magnitude and the diffraction pattern at small scattering angles of t-channel calculations, while the collinear approximation gives a better description of the t-channel diffraction pattern, without, however, reproducing the t-channel order of magnitude ( $f_{coll} \ll 1$  in the legends).

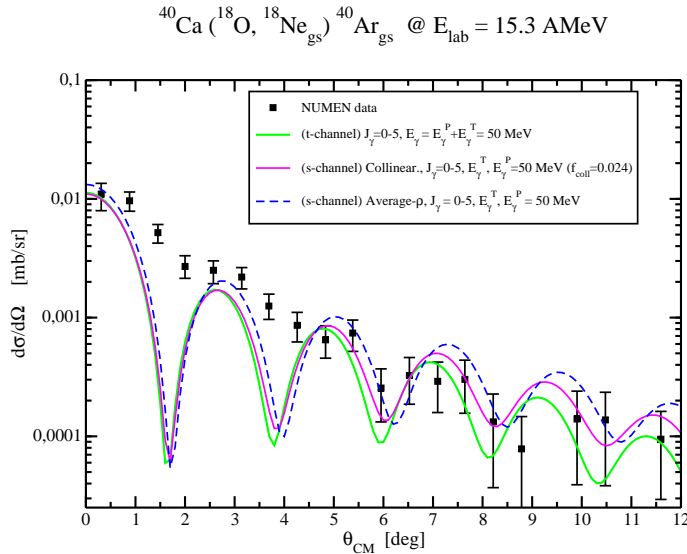


**Figure 1.** Comparison between t-channel (light green line) and s-channel (average- $\rho$  and collinear approximations) DWBA DSCE angular distributions for the reaction  $^{40}\text{Ca}(^{18}\text{O}, ^{18}\text{Ne}_{gs})^{40}\text{Ar}_{gs}$  at 15.3 AMeV. NUMEN data are also shown [2].

Fig.1 also shows the experimental angular distribution, measured by the NUMEN collaboration [2]: for this test DCE reaction, (t-channel) DSCE calculations allow to recover the

order of magnitude and the trend of the data. Of course, to make a reliable comparison with DCE data, it is necessary to coherently sum the contribution from all the possible reaction mechanisms, i.e., the DSCE mechanism described here, the MDCE reaction mechanism and the multi-nucleon transfer feeding DCE, even if the latter is expected to be negligible for the nuclear systems studied [6, 7].

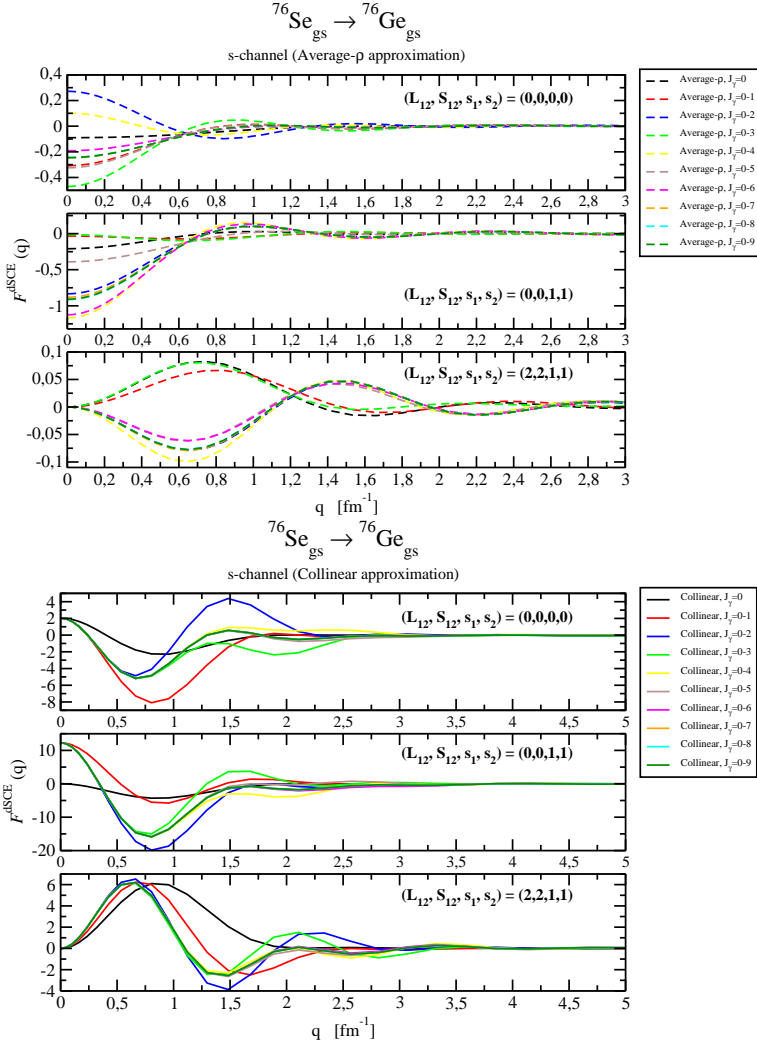


**Figure 2.**  ${}^{76}\text{Se}$  two body radial transition densities as a function of two-step linear momentum transfer  $q$ , for different intervals of  $J_\gamma$ . Upper panel shows average- $\rho$  calculations, while lower panel illustrates results within the collinear approximation. These 2BTDs are evaluated integrating up to  $E_\gamma^T = 50$  MeV.

Similarly, for  ${}^{76}\text{Se}({}^{18}\text{O}, {}^{18}\text{Ne}_{\text{gs}}){}^{76}\text{Ge}_{\text{gs}}$  DSCE angular distributions, the collinear approximation result needs a huge scaling to reach the first maximum of the t-channel angular distribution, while the average- $\rho$  approximation allows to reproduce t-channel order of magnitude,

$^{76}\text{Se}(^{18}\text{O}, ^{18}\text{Ne}_{gs})^{76}\text{Ge}_{gs}$  @ 15.3 AMeV

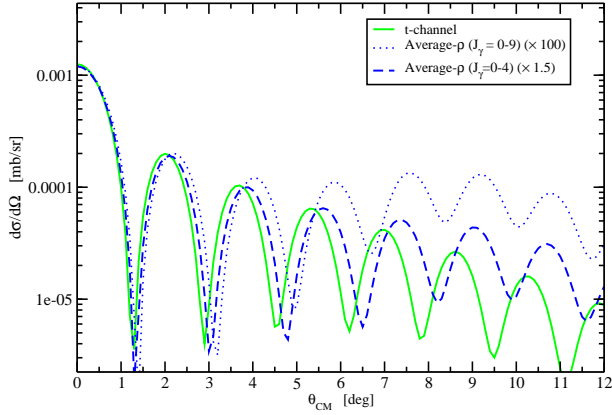


**Figure 3.** Comparison among t-channel (light green line) and s-channel (average- $\rho$  approximation) DWBA DSCE angular distributions for the reaction  $^{76}\text{Se}(^{18}\text{O}, ^{18}\text{Ne}_{gs})^{76}\text{Ge}_{gs}$  at 15.3 AMeV.

trend and diffraction pattern at small scattering angles ( $\theta \lesssim 6^\circ$ ), with the caveat of not including transitions of too high multipolarity in the intermediate channel (see fig. 3).

The trend and diffraction pattern of s-channel calculations can be understood looking at the contributions of each total angular momentum  $J_\gamma$  to the 2BTDs of projectile and target nuclei, within the two approximations discussed above. Fig. 2 illustrates 2BTDs for the target nucleus  $^{76}\text{Se}$  ( $^{76}\text{Se}_{gs} \rightarrow ^{76}\text{Ge}_{gs}$  two-step transition); upper panel refers to average- $\rho$  calculations and lower panel to the collinear approximation. Each of the two panels in fig. 2 contains three plots, illustrating the 2BTDs for the three possible combinations of two-step orbital angular momentum transfer,  $L_{12}$ , SCE and two-step spin transfers,  $S_1, S_2$  and  $S_{12}$ , respectively, contributing to the  $0^+ \rightarrow 0^+$  DCE transition studied.

Fig. 2 illustrates that the collinear approximation strongly suppresses contributions from multipolarities higher than  $J_\gamma = 1$ , at  $q = 0$ , and  $J_\gamma = 3$  for larger values of the two-step linear momentum transfer  $q$ . Instead, within the average- $\rho$  approximation high multipolarities are less suppressed already for small linear momentum transfer values (significant contributions come from high multipolarities, such as  $J_\gamma = 4, 5$  already at  $q = 0$ ). Similar results are obtained for projectile 2BTDs and for the lighter target nucleus,  $^{40}\text{Ca}$ . In [9] it is proved that t-channel results accounts for more  $J_\gamma$  contributions than the collinear approximation. Hence, on the one side, the strong suppression of high multipolarity intermediate channel transitions, together with the small values of  $f_{coll}$ , makes the collinear approximation less reliable than average- $\rho$ . On the other side, the full separation of projectile and target degrees of freedom, through the whole two-step process, leads to a smoother suppression of high multipolarity contributions within the average- $\rho$  approximation than within the t-channel representation. Thus, the average- $\rho$  approximation can be considered more reliable if calculations are extended at most up to the same  $J_\gamma$  value leading to convergent results within the t-channel representation.

Accounting for high multipolarity transitions within the intermediate reaction channel has a big impact on the average- $\rho$  DSCE angular distribution: fig. 3 clearly illustrates that considering multipolarities up to  $J_\gamma = 4$ , the average- $\rho$  approximation nicely reproduces the t-channel angular distribution, while adding higher multipolarities, e.g. up to  $J_\gamma = 9$ , leads

to results that do not recover the correct order of magnitude and that, in the region  $\theta > 6^\circ$ , present a bump and a shift of the minima towards higher  $\theta$  values with respect to the t-channel angular distribution.

To summarize, the average- $\rho$  approximation leads to a reliable factorized expression of the DSCE angular distribution, with the caveat of excluding spurious contributions from high multipolarity nuclear states populated in the intermediate channel.

## 4 Outlooks and Conclusions

HIDCE reactions are described as two-step processes within second order DWBA. A proper extension of the s-channel formalism illustrated in [10], adopting the average- $\rho$  or the collinear approximation, allows to get quite simple expressions of projectile and target 2BTDs and two-step NN interaction potential. Both approximations allow to get an expression of DSCE TME (and thus of DSCE cross section), where projectile and target NMEs appear separately. This interesting result represents a first step towards the extraction of information on double beta decay-like NMEs, once the contributions from all the possible reaction mechanisms are coherently accounted for. In particular, the average- $\rho$  approximation, within the s-channel representation of the DSCE reaction, leads to reliable results, showing small discrepancies, which are under control, with respect to the pilot calculations, i.e. the ones obtained within the t-channel representation.

However, further improvements of the present formalism are in progress. Moreover, it is necessary to improve the nuclear structure inputs used (check of nuclear deformation effects, use of nuclear structure inputs better reproducing the available experimental nuclear energy spectra, for instance). Furthermore, the use of different nuclear structure models (QRPA, Shell Model, IBM, etc.) is envisaged and the coherent sum of all the reaction mechanisms feeding DCE (once available) should be performed. The extension of the DSCE calculations to  $0^+ \rightarrow J^\pi$  DCE reactions, with  $J^\pi \neq 0^+$ , is also a task in progress.

## References

- [1] K. Kisamori *et al.*, Phys. Rev. Lett. **116**, 052501 (2016).
- [2] F. Cappuzzello *et al.*, Eur. Phys. J. **A54**, 72 (2018).
- [3] M. Agostini *et al.*, Rev. Mod. Phys. **95**, 025002 (2023).
- [4] N. Shimizu *et al.*, Phys. Rev. Lett. **120**, 142502 (2018).
- [5] E. Santopinto *et al.*, Phys. Rev. C **98**, 061601 (R)(2018).
- [6] H. Lenske, F. Cappuzzello, M. Cavallaro and M. Colonna, Prog. Part. Nucl. Phys. **109**, 103716 (2019).
- [7] J.A. Lay, S. Burrello, J.I. Bellone, M. Colonna and H. Lenske, within the NUMEN collaboration, *Double Charge-Exchange Reactions and the effect of transfer*, IOP Conf. Series: Journal of Physics: Conf. Series **1056**, 012029 (2018).
- [8] H. Lenske *et al.*, Progress in Particle and Nuclear Physics **109**, 103716 (2019).
- [9] J.I. Bellone, S. Burrello, M. Colonna, J.A. Lay and H. Lenske, Phys. Lett. B **807**, 135528 (2020).
- [10] H. Lenske, J.I. Bellone, M. Colonna and D. Gambacurta, Universe **7** 4, 98 (2021).
- [11] H. Lenske, J.I. Bellone, M. Colonna and J.A. Lay, Phys. Rev. C **98**, 044620 (2018).
- [12] L.C. Chamon *et al.*, Phys. Rev. C **66**, 014610 (2002).
- [13] M. Cavallaro, J.I. Bellone *et al.*, Front. Astron. Space Sci. **8**, 659815 (2021).
- [14] L. La Faiuci *et al.*, Phys. Rev. C **104**, 054610 (2021).